Recovery of cadastral boundaries with GNSS equipment

Recovery of cadastral boundaries with GNSS equipment

A. Cina, A. M. Manzino* and G. Manzino

The purpose of this work is to propose a new redefinition of cadastral boundaries using GNSS equipment and cadastral maps. These maps are the 'original' maps of the Italian Land Cadastre, the first cartographic support built directly from measures carried out by technicians during implantation of the Italian land cadastre. They are called 'originali di impianto' – 'originals of implantation' or 'implant maps'. As such, these maps are valuable and are kept with great care. Recently, the Italian cadastre has carried out an accurate digitisation of these maps in a raster format at a high resolution. In this work, the authors propose the use of these digital maps for the recovery of cadastral boundary. The original cadastral map, one of the primary sources relied upon in defining legal boundaries, generally uses the Bessel ellipsoid localised in Genova and the Cassini-Soldner projection; the GNSS equipment, on the other hand, uses the geocentric ellipsoid with global or continental realisations. After an RTK positioning, the receivers usually provide the cartographic coordinates in a Gauss projection. However, our study deals with the problem of using different projections and reference systems within the limits of a map. In this context, the transition between systems and projections can be made through a conformal transformation with deformations slighter than graphical errors in the map. The difficulty of finding identifiable points in both reference systems is partially solved through a new way of carrying out the redefinition of boundaries by exploiting geometric information.

Keywords: Cadastral boundaries, GNSS, Maps, Conformal transformation, Geometrical constrains

Introduction

Recovery of cadastral boundaries

In the absence of any other reference, one of the documents legally accepted to establish (or rather re-establish) property boundaries is the original cadastral map or 'implant map'. It is known, however, that the reference systems and cartographic projections of these maps are often not the same as those available in real time in a GNSS RTK positioning. The authors indicate the cartographic coordinates of these projections in the two reference systems, respectively, with 'C' (Cadastre) and 'G' (GNSS); improperly, but for brevity and convenience, they call them coordinate systems or 'systems'. The transformation between the two different 'systems' is a complex problem that has already been investigated by several authors (Bildirici, 2003; Bin and Chai, 1996; Cina *et al.,* 2012a, 2012b; Felus, 2007).

The study proposed here addresses this problem in an area limited to a map sheet or a portion of it. This allows for the simplification of the transformation model to a simple roto-translation with scale variation between known points in both systems. This simple solution, however, shows a practical problem that is not negligible, especially when using the implant maps. The transformation between reference frames is only possible when there are a sufficient number of points identifiable on the map and on the ground called 'double points'. It is then necessary to measure the coordinates of these points on the map and on the ground. They are usually indicated by boundary stone markers, many of which have been lost over time. The new way of recovering cadastral boundaries uses additional geometric information of 'belonging' and 'parallelism' to boundaries to perform the transformation between systems.

After a section that introduces the operating modes, the authors develop the basic equations and study the accuracies obtainable.

To verify the correctness of the proposed method, some simulations were performed with the aim of estimating the parameters of roto-translation and the positioning accuracy of points for the recovery cadastral boundaries. In these simulations, the authors show that these points have coordinates with standard deviation more or less comparable with the graphical error of this map. As such, the proposed procedure is feasible in practice. For convenience, the authors refer to the problem of boundary recovery in Italy and give some brief notes on the Italian geodetic and cartographic

Politecnico di Torino, DIATI, Corso Duca degli Abruzzi 24, 10129, Torino, Italy

*Corresponding author, email ambrogio.manzino@polito.it

Received 2 December 2014; accepted 26 January 2015

DOI 10.1179/1752270615Y.0000000007

reference systems. The procedure is, however, general and adoptable for any reference system and mapping in other countries.

Reference system and projection of cadastral map

Let us refer to the original cadastral map. In the absence of other documentation, it is the document that legally allows for the recovery of cadastral boundaries (Angelini, 2008). The maps consulted are not the original cadastral maps. They are constantly updated, but have undergone alterations over time and suffered tears and substantial degradation. The vector maps are derived from scans of the latter for subsequent vectorisation. In Italy, most of the surveys that gave rise to these maps were referred on a Bessel ellipsoid, locally oriented in Genova, with the Cassini-Soldner projection.

Initially, the projections were extended for only a few miles. Later, the limits were extended to the maximum, a distance of 70–80 km away. Within this area, you can replace the local sphere by the ellipsoid. The Cassini-Soldner map projection was used even before its implementation in Italy, for the construction of the old map of France at 1:86 400 scale. Started by Cesare Cassini and continued by his son Giacomo, these maps was finished in 1709 by nephew Domenico. A century later, in 1810, J. Soldner introduced some improvements to the formulae; this updated projection was used to map the Bavarian cadastre. The initiative was then followed by several German states.

The calculation of coordinates in Cassini-Soldner projections starts from a reference system with origin O′. Its geographical coordinates φ_o and λ_o are known on the ellipsoid. The cartographic coordinates of a generic point P′, which has geographic coordinates φ and λ, correspond to the rectangular geodetic coordinates X_P and Y_P of P′ with respect to O′ (Fig. 1). In the cadastral maps, the *X*-axis corresponds to the meridian on the ellipsoid called the central meridian; it passes through the point O′. The *Y*-axis is geodesic perpendicular to *X* in Q′.

The Cassini-Soldner projection is afilactic (neither conformal nor equivalent), but, if the distance from the origin is within 70 km, the representation can be considered equivalent in practice. At this distance, the linear strain has a maximum value of 6 cm km$^{(1}$ in the direction of the meridian, while it is null in the direction of the parallel.

The Italian Cadastre adopted Cassini-Soldner representations in 1886. Only recently, in 2011, did the Italian Ministerial law provide for the adoption of the ETRF2000 reference system. The Italian cadastral system is adjusting to these new rules.

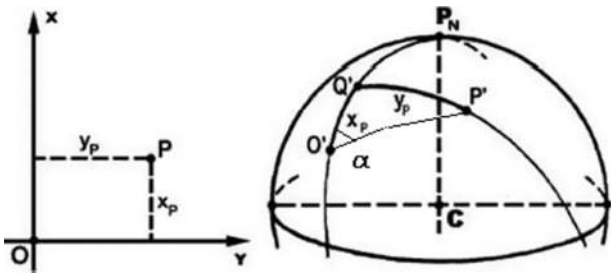

1 Cassini-Soldner projection: *X* and *Y* coordinates

New proposed method

The fundamental problem in the use of GNSS equipment in the recovery of cadastral boundaries is because of the diversity of reference systems and projections (Di Filippo, 2003). The original cadastral map uses an ellipsoid locally oriented and Cassini-Soldner projections, while the GNSS equipment uses the geocentric WGS84 ellipsoid and normally provides coordinates in Gauss projection after an RTK positioning. For brevity, the authors denote the two systems and the two projections with C (Cadastre) and G (Gauss), respectively. As demonstrated by Cina *et al*., (2010a, 2010b), if the size of a survey on the ground is on the order of the size represented by one map (1–2 km), the link between the two reference systems can be modelled, with negligible residual deformations, through a two-dimensional (2D) roto-translation with scale variation. This is the case even when the origin of the cadastral reference system is far from the area of GNSS surveying.

The parameters of this model can be derived if the coordinates of at least two 'double points' in both reference systems are known. Generally, a greater number of points will result in a more correct estimation. Usually, the problem at hand is precisely the search for such points – identified by rectangular stone markers placed between contiguous properties (Fig. 2 *a* and *b*) – or for ideal points consisting of the crossing of axis roads, intersections between roads and canals, bridges and canals or other artefacts found on the ground and in the map (Fig. 6). From the metric point of view, the implant map is also the more precise cartographic support available in the absence of direct surveys (new subdivisions, original sketches, etc.). The only problem is that these implant maps have never been updated; indeed, by definition, the only extant originals should not be subject to changes. The implant map represents the existing boundary lines from more than a century before the advent of GNSS measurements.

At the time of the construction of the map, many dividing lines were evident on the ground; these were based on parallelepipeds that, over time, have been destroyed or uprooted and on which it would be possible, often only in theory, to make GNSS measurements.

Overlapping 'original maps' with aerial images

The lack of availability of 'double points' can be alleviated by means of a new methodology for estimating the parameters of conformal transformation starting from new geometric constraints.

However, we must check in advance onsite if the other geometric information contained in the map can still be found.

In many cases, for this purpose, Google Earth® is a valuable aid because it provides a fairly well-updated aerial image of the territory of the entire globe (Fig. 3).

Note that this overlap does not have metrical meaning, but only serves to allow for the observation of what currently exists in the area that can be recognised on the map.

The first step is the superposition of the original map and the aerial image of the same area. This operation is not trivial, as it requires the cadastral map to be in the same reference system and in the same projection as the image taken from Google Earth, but this is precisely the problem to be addressed. To do this, we can proceed with three approximations:

2 Boundary stone marker buried, found with GNSS measurements; boundary stone found on the ground

- a coarse display area corresponding to the cadastral map, searching for any extant entities
- the use of vector cadastral maps. In Italy, these maps are less accurate than the original maps and are undergoing a slow but steady process of change of reference system in recent years to be consistent with measurements made with GNSS receivers. It will be necessary in this case to clearly distinguish the new boundaries, given the vector maps, from forms already on the original map
- the use of some interpolative approximate methods as we can see in Ching-Sheng and Dah-lih (2003) and Doytsher and Hall (1997).

In Fig. 3 are shown examples of overlapping vector maps with aerial imagery in Google Earth. Figure 4 shows that it is possible to observe how some boundaries have not varied in time, while others appear shifted in parallel to the original map (Fig. 5 *a* and *b*). A classic example of a boundary varied parallel to itself is the shape of a road that has expanded over time, but kept its direction unchanged.

If the aerial image shows a dividing element (a road or a channel) that is present in the map and confirmed on site, a surveyor can measure the coordinates on the ground of some points belonging to these dividers. This is the case even if the divider does not begin or end in the area, or if the stone marker is no longer retrievable on site.

In cases in which the divider has not changed from the original cadastral map, the coordinates (X, Y) of two points along the cadastral boundary detected on the ground by the GNSS receiver can be measured. They can be recorded as coordinates (E, N) in the second reference system (G), for one or more points belonging to this divider. The operation is achievable because the divider is still detectable on the ground (Fig. 4).

The geometric condition of parallelism between two lines is usable in the case where the overlap of the aerial image with the implant map reveals that the divider has changed its position in time parallel to itself (conditions to be checked on site). In this case, first digitally acquire the coordinates in the reference system C of two points constituting the cadastral boundary identified; on the ground, measure the coordinates in the second system G of two points forming the parallel to the divider identified (Fig. 5*a* and *b*).

Examples of parallelism are easy to find in streets or rivers and long straights, which remain unchanged in their direction for centuries.

Finally, it is still possible and useful to investigate 'double points' that are measurable in both reference systems.

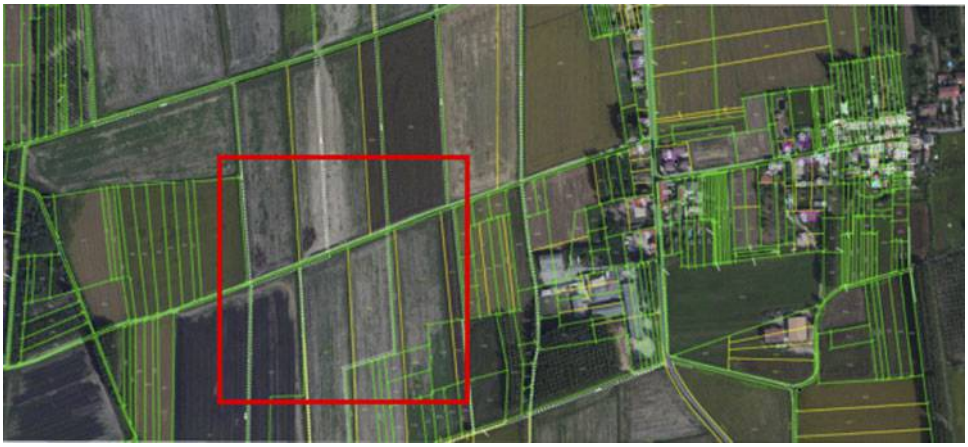

3 Example of overlapping vector cadastral map with aerial image. Original scale map 1:2000

4 Condition of belonging. Measurement of the coordinates on the map (yellow line) and in the field (point P_3)

Even more than in the previous cases, the search for such points requires an inspection of the area, as they are usually invisible from aerial images. In the absence of stone markers, or artefacts on the boundaries, the points that are known in the two frames resulting from the intersection between two dividing lines (roads, a road axis intersecting dividing divider, the intersection of streets and canals in the centre of the bridge, etc.) can be used as control points. Figure 6 shows two examples of 'double points' that can be used on the ground: a stone marker found on the ground (yellow circle) and an intersection of rural road axes (blue circle).

The geometric conditions described above will now be explained mathematically by means of equations.

Estimate of parameters of 2D conformal transformation

From this point, the authors designate as (E, N) the cartographic coordinate in the reference 'G' used by the measure instrumentation system (coordinate visible on the controller of the GNSS receiver or on that of the total station) and designate as (X, Y) the coordinate read on the cadastral map, typically the implant map in a digital raster format.

This last map format is consistent with the reference system and the projection used during the building of cadastral cartography, using a reference system 'C'. Assume that, between the two systems, in limited area interior to a map, we can model the direct and inverse transformation between systems with a 2D four parameter transformation described by the formula

$$\begin{pmatrix} X \\ Y \end{pmatrix} = \begin{pmatrix} X_0 \\ Y_0 \end{pmatrix} + \lambda \begin{bmatrix} \cos\vartheta & sin\vartheta \\ -sin\vartheta & \cos\vartheta \end{bmatrix} \begin{pmatrix} E \\ N \end{pmatrix} \tag{1}$$

The parameter estimation of translation, scale and rotation is immediate in the case where it is possible to find the coordinates of some 'double points' in the two systems C and G. The system is not linear, but it becomes so with a simple change of variables

$$a = \lambda \cos\vartheta; \quad b = \lambda sin\,\vartheta \tag{2}$$

Then (1) becomes

$$\begin{pmatrix} X \\ Y \end{pmatrix} = \begin{pmatrix} X_0 \\ Y_0 \end{pmatrix} + \begin{pmatrix} a & b \\ -b & a \end{pmatrix} \begin{pmatrix} E \\ N \end{pmatrix} = \begin{pmatrix} X_0 \\ Y_0 \end{pmatrix} + B \begin{pmatrix} E \\ N \end{pmatrix} \tag{3}$$

From the solution of these linear equations is then possible to derive

$$\lambda = \sqrt{a^2 + b^2}; \quad \vartheta = \arctan\frac{b}{a} \tag{4}$$

As is well known, it is necessary to have at least four equations, that is, at least two double points to derive the parameters; in practice, it is better to have more than two common points, for which the problem is solved by the least squares.

Since the system is linear in the new unknowns, we can set their approximate values equal to zero. For each point, the known terms are the X and Y coordinates of each point in the system C. Assuming that the coordinates (E, N) in the G system have much better accuracy than the coordinates (X, Y) in the system C and that the scale factor is close to one, both equations can be

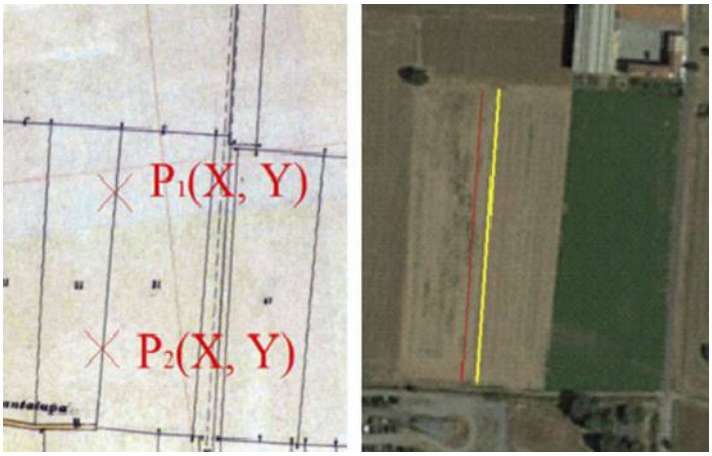

5 Cadastral boundary on the map (a) with its parallel marked on ground (b)

6 'Double points', measurable in both frame systems

weighted with a weight p; this is the inverse of the graphical square error associated with the map scale.

When we subtract the mean coordinates of all the points from the coordinates of the two systems, the least-squares problem can be solved in a closed expression form. In this case, we express the coordinates of the points with respect to the barycentric systems with lower-case letters, i.e.

$$\begin{aligned} x_i &= X_i - X_G; \quad y_i = Y_i - Y_g; \\ e_i &= E_i - E_G; \quad n_i = N_i - N_G \end{aligned} \tag{5}$$

where with X_G, Y_G, E_G, and N_G, we have defined the mean value of the respective coordinates (barycentric coordinates).

With simple algebraic manipulation, we get

$$a = \frac{\sum_{i=1}^{n}(x_i e_i + y_i n_i)}{\sum_{i=1}^{n}(e_i^2 + n_i^2)}; \quad b = \frac{\sum_{i=1}^{n}(x_i n_i - y_i e_i)}{\sum_{i=1}^{n}(e_i^2 + n_i^2)} \tag{6}$$

In these barycentric systems, the two translation values x_0 and y_0 are exactly zero. It is possible to derive the unknown parameters without necessarily having known points in both reference systems, using the condition of a measured point belonging to a segment that represents a cadastral boundary recognised on the ground. The authors denote with (E, N) the coordinate of the point P in the G system and with (X, Y) its coordinates in the C system. They start from the equation of a line through two points P_1 and P_2 (Fig. 7)

$$\begin{aligned} &\frac{X - X_1}{X_2 - X_1} = \frac{Y - Y_1}{Y_2 - Y_1} \quad \Rightarrow \\ &(X - X_1)(Y_2 - Y_1) - (Y - Y_1)(X_2 - X_1) = 0 \end{aligned} \tag{7}$$

The coordinate of the point P can be derived from equation (3). A point belonging to a dividing line generates a single measurement equation

$$\begin{aligned} &(X_0 + aE + bN - X_1)(Y_2 - Y_1) - (Y_0 + aN \\ &\quad - bE - Y_1)(X_2 - X_1) = 0 \end{aligned} \tag{8}$$

The system is still linear in the four unknowns X_O, Y_O, a, and b, for which the approximated values may still be

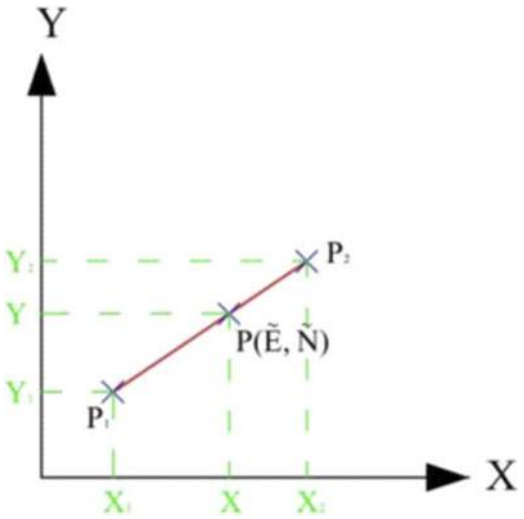

7 Condition of a point belonging to a segment

assumed to be equal to zero. The derivatives with respect to the unknowns X_O, Y_O, a, and b become

$$\begin{aligned} &\tfrac{\partial f}{\partial X_0} = Y_2 - Y_1; \quad \tfrac{\partial f}{\partial Y_0} = -(X_2 - X_1) \\ &\tfrac{\partial f}{\partial a} = E(Y_2 - Y_1) - N(X_2 - X_1) \\ &\tfrac{\partial f}{\partial b} = E(X_2 - X_1) + N(Y_2 - Y_1) \end{aligned} \tag{9}$$

and the known term in the equation is

$$l_0 = X_1 Y_2 - Y_1 X_2 \tag{10}$$

Note that the addition of another measured point on the same alignment (E_2, N_2) does not change the coefficients of the first two columns of the design matrix, involving the translations, or even the known term l_0. In fact, the problem remaining is how to weight these equations. This problem, however, obscures the fact that these equations should be solved with the implicit form of the least-squares method, involving equations of the form

$$g(y + v, x) = 0 \tag{11}$$

In these cases, it is necessary to calculate the matrix of derivatives of the implicit function with respect to the measures that, because the coordinates (E, N) have negligible errors, are the coordinates (X, Y). The derivatives in our case are

$$\begin{aligned} -D = \frac{\partial g}{\partial y} &= \begin{bmatrix} \frac{\partial g}{\partial X_1} & \frac{\partial g}{\partial Y_1} & \frac{\partial g}{\partial X_2} & \frac{\partial g}{\partial Y_2} \end{bmatrix} \\ &= [\,-Y_2 \quad X_2 \quad Y_1 \quad -X_1\,] \end{aligned} \tag{12}$$

The problem is solved in practice by the adoption of a new weight matrix P

$$\bar{P} = (DC_{XY}D^T)^{-1} \tag{13}$$

Considering that for each 'belonging condition', equation (13) is a scalar and that the C_{XY} matrix is proportional to the identity matrix, for these types of measurements, we can use new scalar weights p

$$\bar{p} = \frac{p}{X_1^2 + Y_1^2 + X_2^2 + Y_2^2} \tag{14}$$

Looking at equation (8), we note that to estimate the parameters X_O, Y_O, a, and b, it is necessary to find at least four alignments and then measure at least four

points belong to them on the ground in system G. In addition to the 'belonging condition', it is possible to use a further geometrical condition: parallelism. This condition, unlike the previous one, utilises those lines shown in the map. These are in addition to the property boundaries, which during the years have undergone parallel change from their original position (or may have changed only in the parallel mode). This is the case of a new building if it has a constant distance from the boundary, a fence with unknown distance from the border, the edge of a canal that has expanded over time and whose centreline cannot be measured, etc.

It will be necessary to identify an alignment and then measure two points. They must both be on the original map and on the probable segment that we assume is parallel on the ground, at a unknown distance, to the alignment identified in the map. As we have described, four points are necessary: 1 and 2 with known coordinates (X, Y) in the system C, and the points P and Q of known coordinates (E, N) in the reference system G (Fig. 8). Knowing these four points, it is possible to derive the measuring equations, starting from the parallelism condition of two straight lines, written in an explicit form

$$\begin{aligned} a'x + b'y + c' &= 0 \\ a"x + b"y + c" &= 0 \end{aligned} \tag{15}$$

Two straight lines in the plane are parallel if

$$a'b'' - a''b' = 0 \tag{16}$$

The straight line equation through points 1 and 2, and P and Q (Figure 8) can be written

$$\frac{X - X_2}{X_1 - X_2} = \frac{Y - Y_2}{Y_1 - Y_2}; \quad \frac{X - X_Q}{X_P - X_Q} = \frac{Y - Y_Q}{Y_P - Y_Q} \tag{17}$$

Recognising and collecting the terms that multiply X and Y indicated in equation (15) with a', b', a'', and b'', we have

$$\begin{aligned} &(Y_1 - Y_2)X - (X_1 - X_2)Y - (Y_1 - Y_2)X_2 \\ &+ (X_1 - X_2)Y_2 = 0 \end{aligned}$$

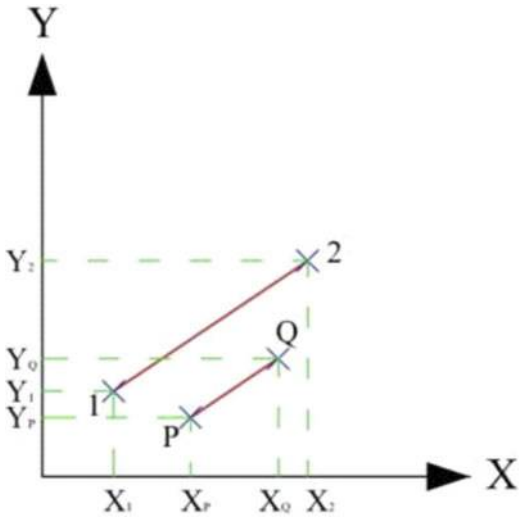

8 Parallelism condition

If we insert the coordinates of the points P and Q

$$\begin{aligned} &(Y_P - Y_Q)X - (X_P - X_Q)Y - (Y_P - Y_Q)X_Q \\ &+ (X_P - X_Q)Y_Q = 0 \end{aligned} \tag{18}$$

The condition of parallelism can then be written as

$$-(Y_1 - Y_2)(X_P - X_Q) + (Y_P - Y_Q)(X_1 - X_2) = 0 \tag{19}$$

Since the points P and Q are known only in the G system, it is necessary to bring them into such a system. For brevity, we denote them as

$$\begin{aligned} \Delta X &= X_1 - X_2; \quad \Delta Y = Y_1 - Y_2 \\ \Delta E &= E_P - E_Q; \quad \Delta N = N_P - N_Q \end{aligned} \tag{20}$$

Recalling (3) we have

$$\begin{aligned} X_P - X_Q &= a\,\Delta E + b\,\Delta N \\ Y_P - Y_Q &= -b\,\Delta E + a\,\Delta N \end{aligned} \tag{21}$$

Substituting in the previous relation the coordinates of the points P and Q in the system C, we use equation (19) to obtain

$$a[-\Delta Y\,\Delta E + \Delta X\,\Delta N] - b[\Delta Y\,\Delta N + \Delta X\,\Delta E] = 0 \tag{22}$$

Again, the equations are linear in the unknowns; however, we note that the two translations have disappeared, implying that they cannot be calculated with this condition. Therefore, we usually have to employ at least some points belonging to an alignment or 'double points' to complete the solution. The partial derivatives with respect to the terms a and b are given in brackets. To this equation is added an important consideration: the equation is homogeneous, i.e. the known term is zero. This means that if one were to use only these measures, we could not compute simultaneously the two terms a and b, but only their ratio. Recalling equation (4), it is understood that the only term that can be calculated is the rotation of the system; the scale factor cannot be determined.

If we had only parallelism equations, the rotation angle between the two systems, the only unknown quantity, would be obtainable in a simple way in a closed form. However, without the unknowns of scale and translations, this formula would not have practical meaning; its only use would be for the theoretical maximisation of the precision of the rotation angle. The good news is that the simulations carried out show that the condition of parallelism, in addition to those 'belonging' and 'double point', improve the accuracy of the rotation angle. It is also useful to remember that this equation, like those corresponding to belonging and double point, must be properly weighted even though the known term is zero. To be precise, it is also necessary here to rewrite the equation implicitly and get the matrix D (the vector D in this case), i.e. the partial derivatives of the function with respect to the coordinates measured in the system C. Observing equation (22), we obtain

$$\begin{aligned} \tfrac{\partial g}{\partial \Delta X} &= a\Delta N - b\Delta E = \Delta Y \\ \tfrac{\partial g}{\partial \Delta Y} &= -a\Delta E - b\Delta N = -\Delta X \end{aligned} \tag{23}$$

and putting p the scalar weight of both coordinates in C system

$$p(\Delta X) = p(\Delta Y) = \frac{p}{2}$$
$$p_{\text{PARALLELISM}} = \frac{p}{2(\Delta X^2 + \Delta Y^2)} \tag{24}$$

To better exemplify the problem, we write the terms of a design matrix A and the vector of known terms l_0 used in the least-squares system

$$Ax - l_0 = v \tag{25}$$

for cases: PD = double point, known in two systems (rows 1 and 2),
AP = belonging to the line (row 3) and
PA = parallelism (row 4).

$$x = \begin{bmatrix} E_0 \\ N_0 \\ a \\ b \end{bmatrix}; l_0 = \begin{bmatrix} X \\ Y \\ X_1X_2 - Y_1Y_2 \\ 0 \end{bmatrix};$$

$$A = \begin{bmatrix} 1 & 0 & E & N \\ 0 & 1 & N & -E \\ Y_2 - Y_1 & X_1 - X_2 & E(Y_2 - Y_1) + N(X_1 - X_2) & E(X_2 - X_1) + N(Y_2 - Y_1) \\ 0 & 0 & (Y_2 - Y_1)(E_P - E_Q) + (X_1 - X_2)(N_P - N_Q) & (Y_2 - Y_1)(N_P - N_Q) + (X_1 - X_2)(E_P - E_Q) \\ \cdots & \cdots & \cdots & \cdots \end{bmatrix} \tag{26}$$

Variance–covariance matrix of coordinates of a point in cadastral system C

It should be remembered that the coordinates used to calculate the parameters of rotational translation are obtained graphically from the map, for which we assume an accidental error equal to the graphical error: 0.2 mm multiplied by the scale factor of the map (0.40 m for the scale 1:2000). The authors assert that the process of recovery of cadastral boundaries is effective if the precision of the vertices found on the ground is still compatible with the accuracy of the map (that is, with its graphical error). For this reason, it is necessary to calculate the variance–covariance matrix of any point in the system C.

To do this, one must consider the dependence of the coordinates from the precision of the input coordinates in the G system, from the position of the point in the G system, and finally, from the precision of the parameters (X_0, Y_0, a, b) derived from the proposed above.

Now the authors rewrite the relation (3) that highlights the dependence of the coordinates (X, Y) in the system C on the coordinates (E, N) in the system G by means of the matrix B.

They now also highlight the link between the coordinates in the C system and the four parameters estimated by the matrix F

$$\begin{pmatrix} X \\ Y \end{pmatrix} = \begin{bmatrix} E & N & 1 & 0 \\ N & E & 0 & 1 \end{bmatrix} \begin{pmatrix} a \\ b \\ X_0 \\ Y_0 \end{pmatrix} = F \begin{pmatrix} a \\ b \\ X_0 \\ Y_0 \end{pmatrix} \tag{27}$$

The variance–covariance matrix of any point in the system C consists of two quantities

$$C_{XY} = BC_{EN}B^T + FC_{abX_0Y_0}F^T \tag{28}$$

The matrix B is made explicit in equation (3).

Assume that the standard deviation of the planimetric coordinates system G is known; if measured in RTK mode, it could be of the order of 2 cm, usually not comparable with the accidental error of the coordinates of the map (Cina *et al.*, 2014; Dabove *et al.*, 2014; Manzino and Dabove, 2013). In this case, C_{EN} is a diagonal matrix with diagonal terms equal to $(0.02\ \text{m})^2$.

To check the compatibility of the precision obtained with the aims of boundary recovery, the authors derive the variance–covariance matrix of five points conveniently located on the map. For these points, they assume the coordinates in the G system to be known. The points were chosen well to be distributed in the map in which the simulations are performed; in particular, four points were chosen at places at the periphery of the map and one point is located approximately in the centre (Fig. 9). The five points under study allow for the simulation of the recovery of the cadastral boundary.

After computing the variance–covariance matrix of the coordinates of each point, we computed the semi-axes of the ellipses error. The aim is to compare the semi-major axis with the graphical error for all the tests and simulations under study. It should be emphasised that the points 2, 3, and 5 are located within the areas of measurement used for the transformation as well as are the only known points in both systems. The points 1 and 4 are intentionally located outside of the area in which they are simulated measurements.

Simulations performed

Preamble

In the previous section, we analysed the equations that govern the various geometrical conditions of our work. To test the operational effectiveness of the equations derived, it is useful to perform a simulation. To achieve this simulation, it was necessary to artificially construct the two coordinate systems. The authors used one 'original cadastral map' of a farming area in Lombardy (Italy), digitalised in the raster format.

The coordinates of the points in the C system were acquired using commercial software on the computer monitor on a georeferenced map, with the use of parametric crosses with known coordinates in Cassini-Soldner projection. On the computer monitor, we have zoomed the digital map to maintain a size on the screen comparable to the scale of 1:2000. The coordinates were then obtained from the mouse position, without the use of 'snap' functions and active with vector maps. In all cases, we assume the collimation error is equal to the accidental graphical error. For each geometrical condition examined (double point, belonging, parallelism and the mixed conditions), more simulations were performed, constructing a series of case studies that, for lack of space, the authors report only partially.

Instead of the coordinates of the measured points in the G system, the same map sheet has been acquired by

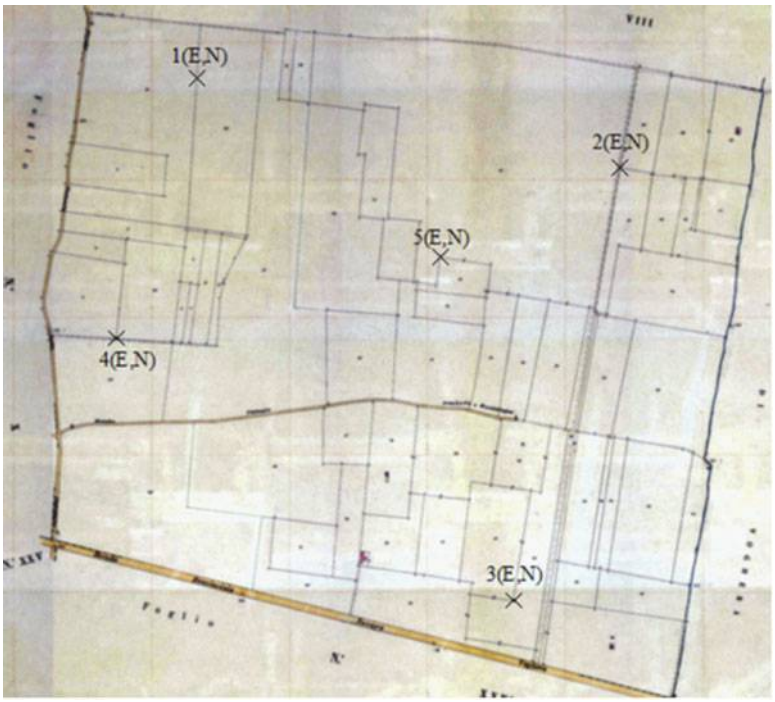

9 Location of the five points of which he wants to know the accuracy. Original scale map 1:2000

CAD through some simple commands. This occurred after rotating and shifting by known quantities

$$X_0 = 100\,\text{m}; \quad Y_0 = 100\,\text{m}; \quad \lambda = 1.00; \quad \vartheta = 30^\circ$$

This has allowed, in the various simulations, for the verification of the accuracy of the results obtained for the estimated parameters. In all the simulations, the authors also calculated and verified the condition number of the normal system. Among the many simulations of measurement, here the authors report the summary results of 10 of them. They only used the 'belonging conditions' (AP hereafter) in some simulations; in others, they included 'parallelism condition' (PA), and in others, the 'double point' condition (PD) is added.

Simulations performed

Table 1 shows the four values of the parameters associated with their mean square error σ. As can be seen, the translations also differ from the imposed values by 5–6 m; the difference comes down to 1 m or less in most redundant schemes. Looking at the σ values of the parameters, it can be argued that the precision obtained is comparable to the accuracy of the results.

However, the result appears poor at the first sight, as we expect an accuracy of a few metres in the values of the offsets (corresponding to an accuracy of a few metres in recovering the cadastral boundary).

Fortunately, this is not the case. If we want to derive the size of the error ellipses on new points, internal or external to the relief, we must take care to correctly propagate accidental errors. The procedure must take into account the variance–covariance matrix, without simplifications – considering, for example, the covariances that play a positive role here (see Table 2).

As we have seen in the previous section, we have calculated the variance–covariance matrix of the points 1, 2, 3, 4 and 5. Table 2 shows the maximum and average values of the semi-major axes of the standard-ellipses on these five significant points. The maximum values were always reached at point 1, outside the ground and, secondarily, at point 4. We note that the maximum values of the semi-major axes range from 57 to 28 cm, values fully comparable with the graphical error for the scale map 1:2000.

Table 1 Values of parameters and accuracies

Case studies	X_O/m, σ/m	Y_O/m, σ/m	Scale λσ (λ)	Rotation ϑ/°, σ/°
Real values	100.00	200.00	1.000	30.00
6 AP	104.923.22	206.604.03	$1.0006.5 \times 10^{-4}$	30.040.03
8 AP	103.331.62	206.752.94	$1.0004.5 \times 10^{-4}$	30.040.02
10 AP	101.292.02	201.793.70	$1.0005.6 \times 10^{-4}$	30.010.03
12 AP	101.311.69	201.982.92	$1.0004.5 \times 10^{-4}$	30.010.02
4 AP + 4 PA	99.184.27	199.195.35	$1.0009.5 \times 10^{-4}$	29.990.04
6 AP + 2 PA	99.184.27	199.195.35	$1.0009.5 \times 10^{-4}$	29.990.04
6 AP + 6 PA	99.821.86	201.082.17	$1.0003.7 \times 10^{-4}$	30.000.02
4 AP + 4 PA + 1 PD	99.183.49	199.194.37	$1.007.7 \times 10^{-4}$	29.990.03
6 AP + 2 PA + 1 PD	99.732.43	200.322.62	$1.0004.7 \times 10^{-4}$	30.000.02
6 AP + 6 PA + 1 PD	99.821.52	201.081.77	$1.0003.0 \times 10^{-4}$	30.000.01

AP: belonging at segment; PA: parallelism; PD: double point, known in both systems.

Table 2 Maximum values and averages of the semi-major axes of the ellipses of error on the points that simulate cadastral boundaries

Case studies	Semi-major axis max value/m	Semi-major axis mean value/m
6 AP	0·57	0·40
8 AP	0·39	0·27
10 AP	0·47	0·34
12 AP	0·37	0·27
4 AP + PA	0·73	0·60
6 AP + 2 PA	0·60	0·36
6 AP + 6 PA	0·35	0·25
4 AP + 4 PA + 1 PD	0·59	0·49
6 AP + 2 PA + 1 PD	0·44	0·39
6 AP + 6 PA + 1 PD	0·28	0·20

AP: belonging at segment; PA: parallelism; PD: double point, known in both systems.

Conclusions

The research described is intended to help the surveyor in all those cases in which he seeks to recover cadastral boundaries. The method, as proposed here in a limited area, is independent of the reference system (local or cartographic) adopted by the measurement equipment and can also be used with measurements acquired by a conventional total station. This algorithm allows for the use of such equipment and is immediate and suitable for handheld controllers or modern topographic or GNSS instrumentation. The procedure can be extended to the group of affine transformations (with six parameters), since the belonging and parallelism conditions are maintained. (This is not the case with projective transformations). These and other issues will be investigated in the future.

Acknowledgement

The authors thank Ing. Tommaso Lacanfora for the simulations carried out as part of his thesis.

References

Angelini, A. 2008. Come fare una riconfinazione. [in Italian]. Available at: <http://www.georoma.it/geopunto/geopunto17/geo17%20p.21%20angelini.pdf>

Bildirici, I. O. 2003. Numerical inverse transformation for map projections. *Computers & Geosciences*, 29, pp. 1003–1011.

Bin, A. Y. and Chai, G. P. 1996. Improving cadastral survey controls using GPS surveying in Singapore. *Survey Review*, 33(261), pp. 488–495.

Ching-Sheng, C. and Dah-lih, W. 2003. Weighted coordinates transformation method for map overlay with non-homogeneous space partition. *Computers & Geosciences*, 29, pp. 877–883.

Cina, A., Caione, S., Chiaffrino, A., Ferrante, F. C., Garretti, L., Manzino, A. M., Pipino, M., Piras, M., Porporato, C. M. and Siletto, G. B. 2012a. La trasformazione di mappe catastali in Regione Piemonte, nel sistema WGS84. *Bollettino della Società Italiana di Fotogrammetria e Topografia*, 1, pp. 9–18, [in Italian]; 11 p.

Cina, A., Ferrante, F. C., Piras, M. and Porporato, M. C. 2012b. La trasformazione dal DATUM catastale ai DATUM Roma 1940 e ETRF2000. *Territorio Italia*, 1, pp. 107–119, [in Italian].

Cina, A., Dabove, P., Manzino, A.M. and Piras, M., Augmented Positioning with CORSs Network Services Using GNSS Mass-Market Receivers, Proceedings of IEEE/ION PLANS 2014, Monterey, CA, May 2014, pp. 359–366.

Cina, A., Manzino, A. M., Porporato, C. and Ferrante, F. C. 2010a. Metodologie geodetiche e cartografiche per la ricomposizione della mappa catastale nel sistema UTM-ETRF2000. *Bollettino della Società Italiana di Fotogrammetria e Topografia*, 1, pp. 27–40, [in Italian].

Cina, A., De Agostino, M., Manzino, A. M. and Piras, M. 2010b. Valorizzazione metrica della mappa d'impianto catastale. *Bollettino della Società Italiana di Fotogrammetria e Topografia*, 1, pp. 41–54, [in Italian].

Dabove, P., Manzino, A. M. and Taglioretti, C. 2014. GNSS network products for post-processing positioning: limitations and peculiarities. *Applied Geomatics*, 6, pp. 27–36.

Di Filippo, S. 2003. Sul passaggio delle coordinate plano-cartografiche dalla rappresentazione di Cassini Soldner al sistema WGS84 e viceversa. *Rivista dell'Agenzia del Territorio*, 1, pp. 85–90, [in Italian].

Doytsher, Y. and Hall, J. K. 1997. Gridded affine transformation and rubber-sheeting algorithm with FORTRAN program for calibrating scanned hydrographic survey maps. *Computers & Geoscience*, 23, pp. 785–791.

Felus, Y. A. 2007. On the positional enhancement of digital cadastral maps. *Survey Review*, 39(306), pp. 268–281.

Manzino, A. M. and Dabove, P. 2013. Quality control of the NRTK positioning with mass-market receivers, in: H. Hsues, (ed.), Global positioning systems: signal structure, applications and sources of error and biases, Nova Science Publishers, Inc. Hauppage, NY, USA, pp. 17–40.